Linear Models for fMRI with Varying Hemodynamics

Firdaus Janoos[1,2], Raghu Machiraju[1,2], Steffen Sammett[2], István Ákos Mórocz[3], Michael V. Knopp[1,2], and Simon Warfield[3]

[1] Dept. of Computer Science, The Ohio State University, USA, janoos.1@osu.edu,
[2] Dept. of Radiology, The Ohio State University, USA,
[3] Dept. of Radiology, Harvard Medical School, USA.

Abstract. In fMRI analysis, linear models are commonly used because of their explanatory power, statistical simplicity and computational efficiency. However, these models make an assumption of a constant hemodynamic response throughout the experiment. Many studies show relatively large variations and non-linearities in the brain hemodynamics, questioning the validity of inferences made with such models. In this paper we present a method which relaxes this assumption, without sacrificing the other advantages of linear models. This method provides estimates of not only the overall activation magnitude and delay, but also the variation in them with respect to experimental conditions. We also validate the statistical properties of our estimator with a simulation study, and show its application on a real fMRI study.

1 Introduction

Functional magnetic resonance imaging (fMRI) is a very powerful tool for studying brain activity by identifying functionally specialized regions and the functional connectivity of the brain. MRI scanners are used to acquire spatio-temporal data, with a time-series at every voxel, which are then used mainly to create maps of activation magnitude [1]. There is also a growing recognition of the need to study the temporal characteristics of the activation, like the delay in the hemodynamic response (HR) to a neurological stimulus, since it provides a more precise and specific mapping of brain function [2, 3].

Though the extent to which the properties of neural activation can be correctly inferred from the measured signal is unknown, it is believed that: 1) a stronger activation leads to an increased BOLD response; 2) a prolonged activation is accompanied by a prolonged response; and 3) a time difference in the activation onset (e.g. between a sensory and an efferent area) is reflected by a temporal shift in the responses of these areas [**?**].

There are many technical impediments in the analysis of fMRI because cortical signal intensity changes are small (¡5%) and there are signal intensity fluctuations due cardiac and respiratory events. The repetition rate of the stimulus is another factor affecting the fMRI time curve as it affects the shape of the hemodynamic response function (HRF) and the duration of the return to baseline. However, under certain conditions, the fMRI response has been found to be approximately linear, indicating that blood oxygenation is linearly coupled to neural activity [**?**].

Most analysis methods [1,4] are based on a linear time-invariant model of brain response formed by the convolution of the stimulus function with an approximate HRF. The parameters of activation are solved for using linear least squares in a General Linear Model (GLM) framework. These models vary in their complexity: early models assumed constant preset values for the response lag and dispersion whereas current models determine these parameters from the data. The response latency at a voxel has been estimated using a first-order Taylor series expansion of the HRF [5] in the GLM. An alternative approach [6] to estimate the activation amplitude and delay uses an orthogonal basis derived from a spectrum of time-shifted HRFs. Estimating the parameters of activation like amplitude, latency, dispersion, etc. through non-linear regression has been variously proposed [7, 8], wherein the estimated HRF is a non-linear function of these parameters. The drawback of such methods is that they require computationally expensive non-linear minimization steps at each voxel. Other linear methods measure the activation onset latency by examining their cross-correlation function with a reference time-series [9]. Such methods do not isolate the component of the signal due to the stimulus of interest, and hence it is unclear how much the latency estimate is affected by confounding factors.

The drawback of all these methods is that they assume a constant (with respect to experimental conditions) hemodynamic response function at each voxel. However, repeated studies have shown a relatively large variation in the observed hemodynamic response, across subjects, across brain sites within the same subject, and even at the same

brain site of the same subject across time [10]. Non-linearities in the transfer from a stimulus to the hemodynamic response have been demonstrated [11], questioning the validity of a time-invariant HRF. Also, the current methods only measure timing differences across voxels, not within the same voxel as experimental conditions change. However, comparison of the response delay makes sense only at the same position in the brain or else it may merely reflect differences in cerebral microvasculature and not of neural recruitment levels [6].

To address these issues, we propose an analysis method that relaxes the assumption of an invariant HRF, without sacrificing the computational efficiency, statistical simplicity and explanatory power of linear models. The delay and magnitude of the hemodynamic response at a particular cortical site is allowed to vary over the duration of the experiment, capturing changes due to changing experimental conditions and subject physiology. In addition, we suggest a low-bias estimator for latency and provide an analytical formulation for its variance, needed for deriving confidence intervals.

The layout of this paper is as follows: In section 2 we present our GLM based method for estimating the activation latency and magnitude at each voxel, without assuming an invariant HRF. Then in section 3 we present a quantitative validation of the statistical properties of our estimator through a simulation study. The application of our method on analyzing a real data-set is shown in section 4. We conclude the paper with a summary of the current method and describe our plans for future work in section 5.

2 Method

Let $s_i(t)$, $i = 1...q$, be the stimulus function representing the onsets and durations of the neurological stimuli corresponding to a task of type i. In conventional analysis of fMRI data, the following two assumptions are made: a) the hemodynamic response is linear; b) the hemodynamic response function is invariant, leading to the following model [12] for the observed signal $y(t)$ at each voxel:

$$Y(t) = \sum_{i=1}^{q} \left[\gamma_i^{(1)} x_1(t) + \gamma_i^{(2)} \dot{x_1}(t) \right] + \varepsilon(t). \tag{1}$$

Here, $x_i(t) = s_i(t) \star h(t)$, $i = 1 \ldots q$ is the expected BOLD response (with no lag) to $s_i(t)$ obtained by convolving it with an typical hemodynamic response function $h(t)$ (For example. see [1]). By including the first-order Taylor series expansion of $x_i(t+\tau) \approx x(t) + \tau \dot{x}(t)$, the model is able to explain a certain amount of delay in the observed response. The coefficient of regressor x_i is $\gamma_i^{(1)}$ and that of $\dot{x}_i$ is $\gamma_i^{(2)}$. The noise term $\varepsilon(t)$ is assumed to be normal, colored, and is typically modeled as an AR(1) process.

In matrix notation, this is $\mathbf{Y} = \mathrm{X}\gamma + \varepsilon$, where X is the $N \times 2q$ design matrix $\mathrm{X} = [\mathbf{x}_1 \dot{\mathbf{x}}_1 \ldots \mathbf{x}_q \dot{\mathbf{x}}_q]$, with $\mathbf{x}_i = (x_i(1) \ldots x_i(N))'$. Also, $\gamma = (\gamma_1^{(1)}, \gamma_1^{(2)}, \ldots \gamma_q^{(1)}, \gamma_q^{(2)})'$ is the coefficient vector, and $\varepsilon = (\varepsilon(1) \ldots \varepsilon(N))'$ is the noise distributed as $\mathcal{N}(0, \sigma_\varepsilon^2 \Sigma_\varepsilon)$. The Gauss-Markov estimate for this system is $\hat{\gamma} = (\mathrm{X}'\Sigma_\varepsilon^{-1}\mathrm{X})^\dagger \mathrm{X}'\Sigma_\varepsilon^{-1}\mathbf{Y}$, and its variance is $\mathrm{Var}[\hat{\gamma}] = \sigma_\varepsilon^2 (\mathrm{X}'\Sigma_\varepsilon^{-1}\mathrm{X})^\dagger$, where $\dagger$ is the pseudo-inverse operation. It can be readily observed that since $x_i(t)$ is orthogonal to $\dot{x}_i(t)$, the covariance between $\hat{\gamma}_i^{(1)}$ and $\hat{\gamma}_i^{(2)}$ is roughly zero indicating that they are almost uncorrelated Gaussian variables, with variance given by the corresponding diagonal elements of $\mathrm{Var}[\hat{\gamma}]$.

For stimulus s_i, the magnitude of the response $\beta_i = \sqrt{(\gamma_i^{(1)})^2 + (\gamma_i^{(2)})^2}$ is estimated by $\hat{\beta}_i = \sqrt{(\hat{\gamma}_i^{(1)})^2 + (\hat{\gamma}_i^{(2)})^2}$ (See [13]). The estimate $\hat{\beta}_i$ has a non-central χ distribution with 2 degrees of freedom and non-centrality $\sqrt{\left(T_i^{(1)}\right)^2 + \left(T_i^{(2)}\right)^2}$, where $T_i^{(k)} = \hat{\gamma}_i^{(k)} / \sqrt{\mathrm{Var}[\hat{\gamma}_i^{(k)}]}$ is the t–score for $\hat{\gamma}_i^{(k)}$ with $k = 1, 2$.

The delay of the response τ_i is related to the ratio of $\gamma_i^{(2)}$ to $\gamma_i^{(1)}$, as [5]:

$$\tau_i \approx \frac{2\alpha_1}{1 + \exp(\alpha_2 \rho_i)} - \alpha_1, \quad \text{where} \quad \rho_i = \frac{\gamma_i^{(2)}}{\gamma_i^{(1)}}. \tag{2}$$

The non-linear transformation of the logistic function was proposed in order to correct for the error due to the neglected higher order terms of the Taylor expansion, and the values its of α_1, α_2 are determined empirically. The unit of τ_i is

in terms of TR, the sampling period. It turns out that the estimate of ρ_i suggested by [5] $\hat{\rho}_i = \hat{\gamma}_i^{(2)}/\hat{\gamma}_i^{(1)}$ is Cauchy distributed and therefore is biased. It also becomes numerically unstable when $\hat{\gamma}_i^{(1)}$ is small.

We provide a solution for this through the following approximation. Since $\hat{\gamma}_i^{(1)}$ and $\hat{\gamma}_i^{(2)}$ are almost independent, $\mathrm{E}[\hat{\rho}_i] \approx \mathrm{E}[\hat{\gamma}_i^{(2)}]\mathrm{E}[1/\hat{\gamma}_i^{(1)}]$. Taking a first order Taylor series expansion of $1/\hat{\gamma}_i^{(1)}$ about $\gamma_i^{(1)}$, and using the fact that it is unbiased, we get:

$$\mathrm{E}[\hat{\rho}_i] = \rho_i \left(1 + \frac{\mathrm{Var}[\hat{\gamma}_i^{(1)}]}{(\hat{\gamma}_i^{(1)})^2}\right) \quad = \hat{\rho}_i \left(1 + \left(T_i^{(1)}\right)^{-2}\right). \tag{3}$$

Therefore, we propose the following corrected estimate for ρ_i as:

$$\hat{\rho}_i^{corr} = \hat{\rho}_i \left(1 + \left(T_i^{(1)}\right)^{-2}\right)^{-1}, \quad \text{giving} \quad \hat{\tau}_i^{corr} \qquad = \frac{2\alpha_1}{1+\exp(\alpha_2 \rho_i^{\hat{corr}})} - \alpha_1. \tag{4}$$

This correction not only un-biases the estimate of the ρ_i but also conditions it numerically when the t–score of $\hat{\gamma}_i^{(1)}$ is low.

To derive an expression for the variance of $\hat{\tau}_i := \tau(\hat{\gamma}_i^{(1)}, \hat{\gamma}_i^{(2)})$, we take a first order Taylor expansion around the true value $\gamma_i^{(1)}$ and $\gamma_i^{(2)}$, and use the fact that their estimates are unbiased to get:

$$\mathrm{Var}[\hat{\tau}_i] \approx \mathrm{Var}\left[\tau(\gamma_i^{(1)}, \gamma_i^{(2)}) + \begin{pmatrix} \frac{\partial \tau}{\partial \gamma_i^{(1)}} & \frac{\partial \tau}{\partial \gamma_i^{(2)}} \end{pmatrix} \begin{pmatrix} (\hat{\gamma}_i^{(1)} - \gamma_i^{(1)}) \\ (\hat{\gamma}_i^{(2)} - \gamma_i^{(2)}) \end{pmatrix}\right] \approx \sum_{k=1}^{2} \mathrm{Var}[\hat{\gamma}_i^{(k)}] \left(\frac{\partial \tau}{\partial \gamma_i^{(k)}}\right)^2. \tag{5}$$

Unfortunately, the model of eqn. 1 can derive only an estimate of average response magnitude β_i and delay τ_i at a given voxel for each stimulus condition s_i, and it fails to characterize the variability of the hemodynamic response within that voxel.

To account for this variability, we partition each stimulus function $s_i(t)$, into a set of p_i stimulus functions $s_{i,j}(t)$, $j = 1...p_i$, such an $s_{i,j}(t)$ represents the stimuli presented when experimental conditions (and subject physiology) could be safely assumed to be constant, thereby justifying the assumption of a constant hemodynamic response. Now, using the partitioned stimulus functions in a GLM we get:

$$Y(t) = \sum_{i=1}^{q} \sum_{j=1}^{p_i} \left[\gamma_{i,j}^{(1)} x_{i,j}(t) + \gamma_{i,j}^{(2)} \dot{x}_{i,j}(t)\right] + \varepsilon(t). \tag{6}$$

In matrix notation, $\mathbf{Y} = \mathrm{X}_a \gamma_\mathbf{a} + \varepsilon$, where $\mathrm{X_a}$ is now an $N \times 2p$ design matrix ($p = \sum_{i=1}^{q} p_i$) containing the partitioned regressors, and γ_a is a vector of the regression coefficients. The original stimulus function $s_i(t)$ is a (weighted) sum of the partitioned stimulus functions $s_{i,j}(t)$, and therefore we can express $\mathrm{X} = \mathrm{X}_a\mathrm{C}$, where $\mathrm{C}_{k,l}$ gives the weight of the k^{th} regressor of $\mathrm{X_a}$ toward the l^{th} regressor of X. It is easy to verify that $\hat{\gamma} = \mathrm{D}\hat{\gamma}_a$, where $\mathrm{D} = \mathrm{C}^\dagger \left(\mathrm{X}_a' \Sigma_\varepsilon^{-1} \mathrm{X}_a\right)^\dagger \left(\mathrm{CC}^\dagger\right)' \mathrm{X}_a' \Sigma_\varepsilon^{-1} \mathrm{X}_a$. It is, however, hard to made inferences from the model of eqn. 6 due the inflated variance of $\hat{\gamma}_a$, caused by increased model degrees of freedom (given by the trace of $\mathbb{P}_{\mathrm{X_a}} = \mathrm{X_a}\left(\mathrm{X_a}'\Sigma_\varepsilon^{-1}\mathrm{X_a}\right)^\dagger \mathrm{X_a}'\Sigma_\varepsilon^{-1}$), and due to an increase in estimate of the noise variance σ_ε^2, caused by reduced residual degrees of freedom. Therefore, to find a tradeoff between the flexibility of the model and its statistical power, we regularize it using the prior belief that the estimates of the coefficients $\{(\gamma_{i,j}^{(1)}\ ,\ \gamma_{i,j}^{(2)})\}_{j=1}^{N}$ are normally distributed around the mean response $(\overline{\gamma}_i^{(1)}\ ,\ \overline{\gamma}_i^{(2)})$ for the stimulus s_i, with variance $\sigma_\gamma^2 \Sigma_\gamma$. Here Σ_γ is a diagonal matrix representing the relative scales of the variation in $\gamma_{i,j}^{(1)}$ with respect to that of $\gamma_{i,j}^{(2)}$. The maximum *a posteriori* estimate for γ_a results in the following ridge-regression formulation:

$$\hat{\gamma}_a(\lambda) = \min_{\gamma} [\mathbf{Y} - \mathrm{X}_a\gamma]' \Sigma_\varepsilon^{-1} [\mathbf{Y} - \mathrm{X}_a\gamma] + \lambda \gamma' \mathrm{Q} \gamma, \tag{7}$$

where $\mathrm{Q} = [\mathrm{I} - \mathrm{DD}^\dagger]' \Sigma_\gamma^{-1} [\mathrm{I} - \mathrm{DD}^\dagger]$. Here, λ represents the ratio $\sigma_\varepsilon^2/\sigma_\gamma^2$. A value of $\lambda = 0$ indicates a flat prior on γ_a, and the solution corresponds to the OLS estimate $\hat{\gamma}_a$ of eqn. 6.

The diagonal values of Σ_γ are estimated by first computing the OLS values of $\hat{\gamma}_a$, and then setting the relative scale of $\hat{\gamma}_{i,j}^{(1)}$ to 1 and that of $\hat{\gamma}_{i,j}^{(2)}$ as the ratio of the empirical variance of $\hat{\gamma}_{i,j}^{(2)}$ to that of $\hat{\gamma}_{i,j}^{(1)}$.

The minimizer to eqn. 7 is $\hat{\gamma}_a(\lambda) = \left(\mathrm{X_a}'\Sigma_\varepsilon^{-1}\mathrm{X_a} + \lambda\mathrm{Q}\right)^\dagger \mathrm{X_a}'\Sigma_\varepsilon^{-1}\mathbf{Y}$. The model degrees of freedom (i.e. trace of $\mathbb{P}_{\mathrm{X_a}}(\lambda) = \mathrm{X_a}\left(\mathrm{X_a}'\Sigma_\varepsilon^{-1}\mathrm{X_a} + \lambda\mathrm{Q}\right)^\dagger \mathrm{X_a}'\Sigma_\varepsilon^{-1}$) is a decreasing function of λ. Through a re-arrangement of the terms, it can be seen that $\hat{\gamma}_a(\lambda) = \mathrm{T}(\lambda)\hat{\gamma}_a$, where $\mathrm{T}(\lambda) = (\mathrm{I} + \lambda(\mathrm{X_a}'\Sigma_\varepsilon^{-1}\mathrm{X_a})^\dagger\,\mathrm{Q})^\dagger$. The mean squared error of the estimate $\hat{\gamma}_a(\lambda)$ can be partitioned as $MSE(\lambda) = \sigma_\varepsilon^2\ \mathrm{trace}\{\mathrm{T}(\lambda)\ (\mathrm{X_a}'\Sigma_\varepsilon^{-1}\mathrm{X_a})^\dagger\ \mathrm{T}(\lambda)'\} + \gamma_a'[\mathrm{T}(\lambda)-\mathrm{I}]'[\mathrm{T}(\lambda)-\mathrm{I}]\gamma_a$, where the first term is the variance and the second is the square bias of the estimator. The optimal value λ^* of λ is chosen as that which minimizes $MSE(\lambda)$, which in the case of linear LS regression is well-approximated by the Cp statistic [14]:

$$Cp(\lambda) = \mathbf{Y}'\left[\mathrm{I}-\mathbb{P}_{\mathrm{X_a}}(\lambda)\right]\mathbf{Y} + 2\frac{\mathrm{trace}\{\mathrm{I}-\mathbb{P}_{\mathrm{X_a}}(\lambda)\}}{N}\frac{\mathbf{Y}'[\mathrm{I}-\mathbb{P}_{\mathrm{X_a}}(0)]\mathbf{Y}}{\mathrm{trace}\{\mathrm{I}-\mathbb{P}_{\mathrm{X_a}}(0)\}}. \tag{8}$$

3 Model Validation

In this section, we present a quantitative validation of the statistical properties of our estimator through a simulation study. The parameters of our experiments are the SNR $= 20\log_{10}\overline{h}/\sigma_\varepsilon$, and the allowed variation in response magnitude and delay characterized by σ_γ. Here, $\overline{h}$ is the RMS power $\sqrt{\sum_t h^2(t)/T}$ of the HRF used. The stimulus function $s_1(t)$ (generated by a Poisson process) was partitioned into $s_{1,j}(t)$, $j = 1...p_1$, and the measurement time-series $y(t)$ was generated as $\sum_{j=1}^{p_1} s_{1,j} \star h_{1,j}(t) + \varepsilon(t)$ where $h_{1,j}(t)$ is the canonical HRF [12] sampled with a period of $TR = 2$–secs, typical of most real fMRI acquisitions. Each individual HRF $h_{1,j}(t)$ was delayed by $\tau_{1,j}$ (in TR units) and amplitude $\beta_{1,j}$ (arbitrary units AU). The $\beta_{1,j}$ and $\tau_{1,j}$ were obtained as functions of $\gamma_{1,j}^{(1)}$ and $\gamma_{1,j}^{(2)}$ sampled from $\mathcal{N}\left((\overline{\gamma}_{i,j}^{(1)}\overline{\gamma}_{i,j}^{(2)}), \sigma_\gamma^2\Sigma_\gamma\right)$. The noise $\varepsilon(t)$ was generated by an AR(1) process with the AR coefficient=0.3 and variance σ_ε^2.

In fig. 1 we show the percentage MSE, variance and squared-bias of the estimates for $\hat{\beta}_{i,j}(\lambda^*)$ and $\hat{\tau}_{i,j}^{corr}(\lambda^*)$.[4] We also

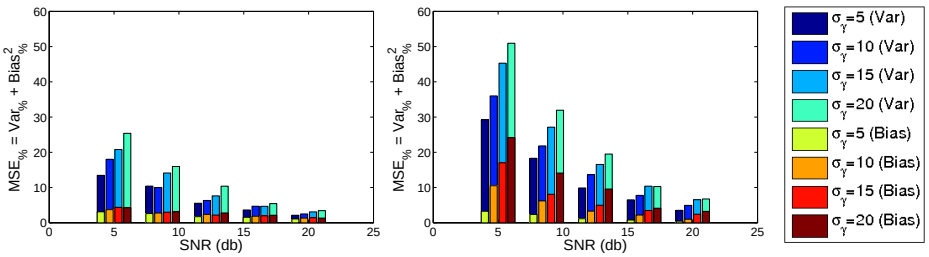

(a) $\hat{\beta}_{i,j}$ (b) $\hat{\tau}_{i,j}^{corr}$ (c) Legend

Fig. 1. The percentage variance, squared-bias, and MSE for the estimates of $\hat{\beta}_{i,j}$ in fig. (a) and $\hat{\tau}_{i,j}^{corr}$ in fig. (b) plotted with respect to SNR. The legend in fig. (c) shows the color coding for the squared-bias and variance components for different values of σ_γ. Note that MSE = Var + Bias^2. For all the estimates, we observe a reduction of bias and variance with respect to increasing SNR and smaller σ_γ. Also, the bias in $\hat{\beta}_{i,j}$ is relatively large compared to its variance. This is due to the fact that $\hat{\beta}_{i,j}$, is a non-central chi variable and therefore inherently biased. However, in absolute terms the bias and the overall MSE is fairly low. Though the MSE for $\hat{\tau}_{i,j}^{corr}$ is fairly high, given the low temporal resolution and SNR of fMRI, it is acceptable, and it drops quickly as the SNR improves.

observed that the bias of our corrected estimator for τ was about 70% less than that of the original estimator of [5], and the empirical variance of $\hat{\tau}^{corr}$ was (1 ± 0.2) times the analytical variance from eqn. 5.

[4] $\mathrm{MSE}_{\%}(\hat{\beta}) = 100\times\mathrm{E}_\beta\left[\mathrm{E}_{\hat{\beta}|\beta}[(\hat{\beta}-\beta)^2]\right]/\left(\mathrm{E}_\beta[\beta]\right)^2$; $\mathrm{Var}_{\%}(\hat{\beta}) = 100\times\mathrm{E}_\beta\left[\mathrm{E}_{\hat{\beta}|\beta}[(\hat{\beta}-\mathrm{E}[\hat{\beta}])^2]\right]/\left(\mathrm{E}_\beta[\beta]\right)^2$; and $\mathrm{Bias}^2_{\%}(\hat{\beta}) = 100\times\mathrm{E}_\beta\left[(\mathrm{E}_{\hat{\beta}|\beta}[\hat{\beta}-\beta])^2\right]/\left(\mathrm{E}_\beta[\beta]\right)^2$.

4 Results

We present some results of our method applied to an fMRI study designed to assess the neural substrates involved in visuo-spatial memory maintenance and manipulation. Each trial started with the display of a 250–ms fixation cross, followed by three nameable objects for 2000–ms each, interleaved with 250–ms fixation crosses. After the last object, the instruction "forward" or "backward" was presented for 1000–ms. Participants were instructed to mentally rehearse or reorder the names of the three objects for a 6,000-ms period. One of the three objects was re-displayed as a probe, and the subjects were required to indicate with a button press whether the probe object was the first, second, or third object in the forward or backward sequence, during another 6000–ms window.
Acquisition was done on a Siemens 3T Tim Trio MRI scanner with a quadrature head coil using a BOLD sensitized 3D-EPI gradient-echo pulse sequence with the following specifications: echo time 30ms, flip angle 30°, volume scan time 2.22s, and voxel size $3 \times 3 \times 3.75$–mm. A typical study lasted around 11 minutes, with about 30 trials. Routine pre-processing (motion and slice-timing correction, spatial normalization to a standard brain space, co-registration of functional and structural scans, and spatial smoothing with an 8–mm Gaussian filter) was done in SPM5 [1].
To test for a change in brain activity with respect to experiment time ($t = 1...T$) and recall direction ($r = 1$ for "forward", $r = 2$ for "backward"), the stimuli were first partitioned into $T \times 1$–min intervals, then further partitioned based on recall direction, thus resulting in $T \times 2$ regressors. The activation magnitude ($\beta_{t,r}$) and delay coefficients ($\tau_{t,r}$) were computed using the model of eqn. 7. First, those voxels exhibiting significant ($\alpha = 0.05$, FDR corrected) mean activity $\overline{\beta}$ were identified. The t-scores of these voxels, for one subject, are shown in fig. 2(a). In fig. 2(b) the average delay in the response at these voxels is shown. The pattern of activation magnitudes and latencies (mainly in the dorso-lateral pre-frontal cortex, intra-parietal sulcus, visual and auditory regions) correspond with the expected brain recruitment for this task [15]. The coefficients were then separately tested for an effect due to the interaction of time and recall direction, by a linear regression against $t \times r$. The correlation coefficient of the regression for $\beta_{t,r}$ is shown in fig. 2(c), and for $\tau_{t,r}$ in fig. 2(d). A positive correlation of $\beta_{t,r}$ with $t \times r$ points to increased neural activity at that region as experiment time increases and when the subject has to do a recall in the backward direction. A positive correlation of $\tau_{t,r}$ with $t \times r$ implies increased sluggishness in the response. Such maps indicate changing hemodynamics which could be due to attention, fatigue, task complexity, or adaptation (learning) effects, and help in making more informative inferences from the data.

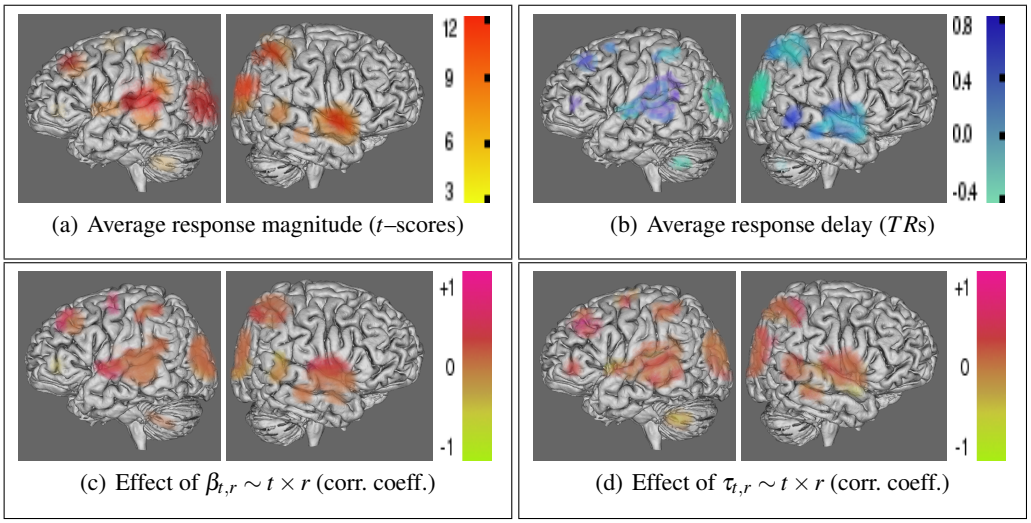

(a) Average response magnitude (t–scores)

(b) Average response delay (TRs)

(c) Effect of $\beta_{t,r} \sim t \times r$ (corr. coeff.)

(d) Effect of $\tau_{t,r} \sim t \times r$ (corr. coeff.)

Fig. 2. Fig. (a) shows the t-scores for mean activation magnitude $\overline{\beta}_{t,r}$ (Left and right hemispheres). Fig. (b) shows the average delay $\overline{\beta}_{t,r}$ (in TR units). The correlation coefficient of the regression line of the magnitude coefficients $\beta_{t,r}$ vs. $t \times r$ is shown in fig. (c) and delay coefficients $\tau_{t,r}$ in fig. (d). Color saturation indicates the depth within the cortical surface.

5 Discussion

In this paper, we have proposed an extension to standard models for fMRI analysis that relaxes the assumption of an invariant hemodynamic response function, while preserving the many advantages of a GLM framework. This not only provides a better model for the data, but also allows us to make more powerful inferences about the effect of different experimental conditions on brain activity. We also developed a low-bias activation latency estimator and derived an analytical approximation of its variance, allowing for statistical tests of significance. We demonstrated the statistical validity of our estimator through simulations, and showed its application on a real fMRI study.
Currently, we are developing methods that can deal with more variation in the hemodynamics through non-parametric representations of the HRF, and that will capture latency effects with higher precision. We are also looking at ways to characterize the variation of all the aspects of the hemodynamic response.

References

1. Friston, K., Holmes, A., Worsley, K., Poline, J., Frith, C., Frackowiak, R.: Statistical parametric maps in functional imaging: A general linear approach. Hum. Brain Map. **2**(4) (1995) 189–210
2. Menon, R.S., Luknowsky, D.C., Gati, J.S.: Mental chronometry using latency-resolved functional MRI. Proc Natl Acad Sci U S A **95**(18) (Sep 1998) 10902–10907
3. Formisano, E., Goebel, R.: Tracking cognitive processes with functional MRI mental chronometry. Curr Opin Neurobiol **13**(2) (2003) 174–181
4. Worsley, K.J., Liao, C.H., Aston, J., Petre, V., Duncan, G.H., Morales, F., Evans, A.C.: A general statistical analysis for fMRI data. Neuroimage **15**(1) (Jan 2002) 1–15
5. Henson, R.N.A., Price, C.J., Rugg, M.D., Turner, R., Friston, K.J.: Detecting latency differences in event-related bold responses: application to words versus nonwords and initial versus repeated face presentations. Neuroimage **15**(1) (Jan 2002) 83–97
6. Liao, C.H., Worsley, K.J., Poline, J.B., Aston, J.A.D., Duncan, G.H., Evans, A.C.: Estimating the delay of the fMRI response. Neuroimage **16**(3 Pt 1) (Jul 2002) 593–606
7. Kruggel, F., Zysset, S., von Cramon, D.Y.: Nonlinear regression of functional MRI data: an item recognition task study. Neuroimage **12**(2) (Aug 2000) 173–183
8. Purdon, P.L., Solo, V., Weisskoff, R.M., Brown, E.N.: Locally regularized spatiotemporal modeling and model comparison for functional MRI. Neuroimage **14**(4) (Oct 2001) 912–923
9. Saad, Z.S., DeYoe, E.A., Ropella, K.M.: Estimation of fMRI response delays. Neuroimage **18**(2) (Feb 2003) 494–504
10. Sirotin, Y.B., Das, A.: Anticipatory haemodynamic signals in sensory cortex not predicted by local neuronal activity. Nature **457**(7228) (Jan 2009) 475–479
11. Boynton, G.M., Engel, S.A., Glover, G.H., Heeger, D.J.: Linear systems analysis of functional magnetic resonance imaging in human v1. J Neurosci **16**(13) (Jul 1996) 4207–4221
12. Friston, K.J., Fletcher, P., Josephs, O., Holmes, A., Rugg, M.D., Turner, R.: Event-related fMRI: characterizing differential responses. Neuroimage **7**(1) (Jan 1998) 30–40
13. Calhoun, V.D., Stevens, M.C., Pearlson, G.D., Kiehl, K.A.: fMRI analysis with the general linear model: removal of latency-induced amplitude bias by incorporation of hemodynamic derivative terms. Neuroimage **22**(1) (May 2004) 252–257
14. Mallows, C.: Some comments on Cp. Technometrics **15** (1973) 661–675
15. Bunge, S.A., Wright, S.B.: Neurodevelopmental changes in working memory and cognitive control. Curr Opin Neurobiol **17**(2) (Apr 2007) 243–250